Journal of Superconductivity and Novel Magnetism (2021) 34:1067–1075
https://doi.org/10.1007/s10948-021-05812-2

ORIGINAL PAPER

New Evidence of Interaction Between Grain and Boundaries Subsystems in Granular High-Temperature Superconductors

D. A. Balaev[1,2] · S. V. Semenov[1,2] · D. M. Gokhfeld[1,2]

Received: 3 December 2020 / Accepted: 21 January 2021 / Published online: 4 February 2021

Abstract
Granular high-temperature superconductors (HTSs) exhibit magnetotransport properties, including the clockwise magnetoresistance hysteresis. The hysteresis is explained by the concept of an effective field in the subsystem of grain boundaries, where the observed dissipation occurs. The effective field in the intergrain medium is determined by a superposition of the external field H and the field induced by the magnetic response of HTS grains. The magnetic flux compression in the intergrain medium provides an increase of the effective field. The magnetoresistance hysteresis of polycrystalline $YBa_2Cu_3O_{7-\delta}$ has a bright feature: In a fairly wide external field range, the hysteresis width $\Delta H(H)$ is found to be almost linear, $\Delta H \approx H$. This behavior is considered to be universal over the entire temperature range corresponding to the superconducting state (the investigations have been carried out at temperatures of 77 K and 4.2 K). The analysis of the magnetoresistive and magnetic properties has shown that the upper boundary of the field range of the $\Delta H \approx H$ regime is consistent with the field of complete penetration into HTS grains. This is indicative of the strong interrelation between the magnetotransport and magnetic properties of granular HTSs.

Keywords Magnetoresistance · Hysteresis · YBCO · Magnetic flux compression · Effective field · Intergrain medium

1 Introduction

Granular high-temperature superconductor (HTS) materials are important for various applications since they exhibit intriguing properties related to their magnetotransport characteristics. The latter results from the implementation of a two-level superconducting system in granular HTSs. On the one hand, there are superconducting grains with a high density of the critical current. The currents in grains, together with the capture of the magnetic flux (Abrikosov vortices), form the magnetic properties of granular HTSs, including their diamagnetism and a characteristic magnetic hysteresis loop. On the other hand, the subsystem of grain boundaries is also capable of transferring the superconducting current due to the Josephson effect, as long as the geometric thickness of the grain boundaries does not exceed the coherence length. The observed dissipation occurs, first of all, in the subsystem of grain boundaries.

The above-described picture was clarified in the first years after the discovery of high-temperature superconductivity [1–7]. Later on, the studies on the magnetotransport properties (electrical resistance vs. temperature in magnetic fields and I–V characteristics) of granular HTSs aimed at the determination of the dissipation mechanisms in the subsystem of grain boundaries were carried out [8–22]. It should be emphasized here that, due to the great difference between the critical currents of the abovementioned superconducting subsystems, the contribution of grain boundaries can be unambiguously distinguished, especially for classical yttrium and lanthanum HTSs.

Meanwhile, some facts were experimentally established that indicated a more complex picture of the magnetotransport phenomena. They were, in particular, the hysteresis of the magnetoresistance $R(H)$ and critical current [23, 24], effect of the thermomagnetic prehistory on the magnetotransport characteristics [25, 26], and anisotropy of the magnetotransport properties relative to the directions of magnetic field $\boldsymbol{H}$ and transport current $\boldsymbol{I}$ (while a granular HTS is macroscopically isotropic due to the random arrangement of anisotropic crystallites forming the sample) [26–32]. This suggested the interaction

✉ D. M. Gokhfeld
gokhfeld@iph.krasn.ru

[1] Kirensky Institute of Physics, Federal Research Center KSC SB RAS, Krasnoyarsk 660036, Russia

[2] Siberian Federal University, Krasnoyarsk 660041, Russia

between the subsystems of HTS grains and intergrain boundaries in granular HTSs [32–37].

The main mechanism of the interaction between the superconducting subsystems in granular HTSs was found to be the effect of the magnetic moments of grains on the field in the intergrain medium. The description of this mechanism gave rise to the concept of an effective field in the intergrain medium of a granular HTS [32–35]. According to this concept, grain boundaries are affected by field $\boldsymbol{B}_{\text{eff}}$, which represents a superposition of the external field and the field $\boldsymbol{B}_{\text{ind}}$ induced by HTS grains (Fig. 1a):

$$\boldsymbol{B}_{\text{eff}} = \boldsymbol{H} + \boldsymbol{B}_{\text{ind}} \tag{1}$$

The value and macroscopic direction of the field $\boldsymbol{B}_{\text{ind}}$ are related to the magnetic properties of grains and, eventually, to the experimental magnetization M, i.e., the $M(H)$ and $M(T)$ dependences: $B_{\text{ind}}(H,T) \sim |M(H,T)|$. Therefore, Eq. (1) can be rewritten in the form

$$B_{\text{eff}}(H,T) = |H - \alpha \cdot 4\pi M(H,T)| \tag{2}$$

Equation (2) has already taken into account the magnetization sign relative to the external field (see Fig. 1a and 1b) and contains the coefficient of proportionality α between the averaged magnetization of grains $4\pi M(H)$ [34, 35] and the induced field $\boldsymbol{B}_{\text{ind}}$.

The $R(H)$ and $B_{\text{eff}}(H)$ interplay is determined using the conventional Arrhenius relation $R(H,T,I) \sim \exp(-E_J(H,T,I)/k_BT)$ [36], where E_J is the energy of the Josephson coupling, but the external field should be replaced by the effective field in the intergrain medium: $B_{\text{eff}}(H) \rightarrow H$ [37]:

$$R(H,T,I) \sim \exp(-E_J(B_{\text{eff}}(H,T),T,I)/k_BT) \tag{3}$$

Thorough investigations of the galvanomagnetic effects in granular HTSs made it possible to describe first qualitatively [30–35, 38–41] and then quantitatively, the mechanisms of the previously unclear properties including the clockwise $R(H)$ hysteresis [42–47], effect of the thermomagnetic prehistory on the $R(T)$ and $R(H)$ dependences [41, 48, 51, 52], and magnetoresistance anisotropy $R(\boldsymbol{H},T,\boldsymbol{I})$ [53, 54]. It was found surprisingly that the parameter α in Eq. (2) has a value of about 10 or more [41, 47, 51–54] (this is mainly true for yttrium and lanthanum HTSs). This is evidence for significant crowding of the flow in the grain boundaries [50–56], which is illustrated in Fig. 1c. In fact, a large value of the parameter α leads to the wide magnetoresistance hysteresis [50–55] and the $R(H)$ hysteresis is observed as long as the $M(H)$ dependence stays irreversible (see Eq. (2)) [46, 48].

This work is aimed to reveal the regularities in the behavior of the magnetoresistance hysteresis of granular HTS in a wide temperature range. Any hysteretic dependence can be characterized by the two main parameters: height and width. In this study, we draw attention to an interesting feature of the $R(H)$ hysteresis in a granular HTS of the yttrium system: the functional dependence of the $R(H)$ hysteresis width on the external field behaves identically at different temperatures (in our experiments, the data were obtained at temperatures from 4.2 K to almost critical temperature T_C). This is apparently another manifestation of the magnetic flux compression

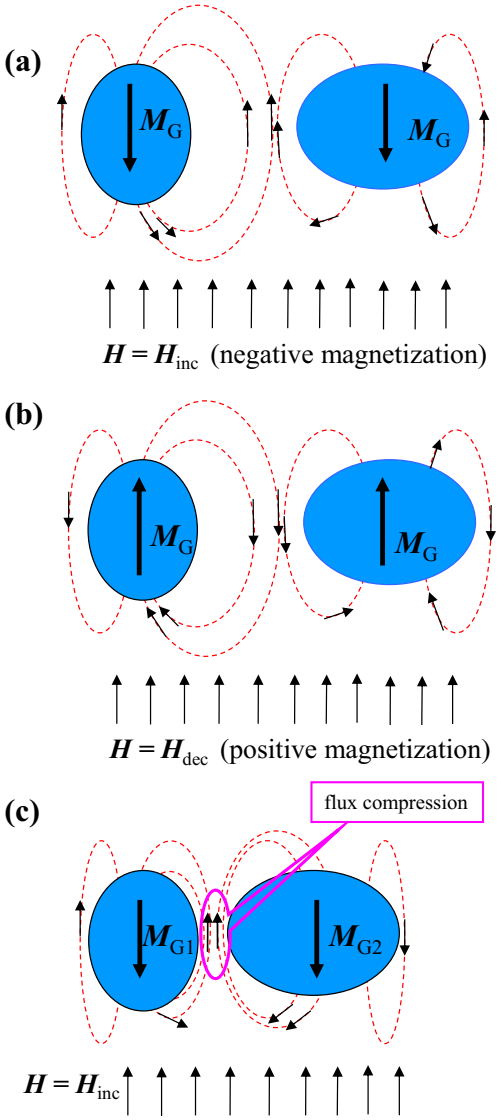

Fig. 1 Schematic of magnetic induction lines in the intergrain medium of a granular HTS. Ovals show HTS grains and the space between them is the intergrain medium; intergrain spacings are significantly enlarged. Dashed lines show the lines of magnetic induction B_{ind} from the magnetic moments M_{G1} and M_{G2} of HTS grains (bold arrows); thin arrows show the B_{ind} direction (**a**) in the increasing external field $H = H_{\text{inc}}$ at the negative magnetization (M_{G1} and M_{G2} are antiparallel to H_{inc}, $B_{\text{ind}} \parallel H_{\text{inc}}$) and **b** in the decreasing external field $H = H_{\text{dec}}$ at the positive magnetization (M_{G1}, $M_{G2} \parallel H_{\text{dec}}$ B_{ind} is antiparallel to H_{dec}). **c** Effect of the magnetic flux compression (compare with (**b**)) observed in real granular HTSs, in which the grain boundary length is several nanometers and the grain size is several micrometers

in the intergrain medium, which is related to the penetration of a field into HTS grains.

2 Experimental

The $YBa_2Cu_3O_{7-\delta}$ HTS sample was obtained by the solid-state synthesis from corresponding oxides with three intermediate grindings. The scanning electron microscopy and energy-dispersive spectrometry data were obtained on a Hitachi-TM 4000 electron microscope. The magnetotransport measurements were performed by a four-point probe technique on a sample with the size of 0.15 × 0.15 × 7 mm^3. An external field H was induced by an electromagnet (at $T \geq 77$ K) or by a superconducting solenoid (at $T = 4.2$ K); H was applied perpendicular to the macroscopic transport current I, which was biased along the major axis of the sample. The $R(H)$ dependences at temperatures of 4.2 K and 77 K were obtained by placing the sample directly in liquid helium or nitrogen, respectively. This was necessary to ensure the effective removal of heat released on the current contacts during the flowing of a current of ~ 300 mA. In all the cases, the sample was cooled in zero external fields (ZFC mode).

The magnetic properties were investigated on a vibrating sample magnetometer under the external conditions (including the external magnetic field sweep rate) corresponding to the magnetotransport measurements.

3 Sample Characterization

According to the results of X-ray diffraction analysis, all the reflections of the obtained samples correspond to an HTS with a 1-2-3 structure; no foreign phases were observed. Figure 2 shows a typical scanning electron microscopy image of the sample microstructure. One can clearly see the granular structure with a grain size from 0.5 to 12 μm. Figure 3 shows the size distribution of grains. The average grain size is ~ 4 μm. According to the energy-dispersive spectrometry data, the elemental composition corresponds to the chemical formula $YBa_2Cu_3O_{7-\delta}$. The physical density of the investigated sample was ~ 86% of the theoretical density of $YBa_2Cu_3O_{7-\delta}$.

Figure 4a presents the temperature dependence of the sample magnetization in a field of H = 100 Oe obtained after meeting the ZFC conditions. According to these data, the transition temperature T_C was ~ 92.8 K.

The resistivity was found to be ~ 15.4 mΩ cm at T = 300 K and ~ 10.3 mΩ cm at T = 100 K. The critical current in zero external fields was ~ 10^2 A/cm^2 at T = 4.2 K and ~ 5 A/cm^2 at T = 77 K. The relatively low density of the transport (intergrain) critical current for this sample is explained by the fact that no special measures (e.g., high-temperature annealing) were taken to increase it.

The temperature dependences of the electrical resistance in zero external field and fields of 10, 100, and 1000 Oe are shown in Fig. 4b. The onset of the resistance drop corresponds to the critical temperature determined from the magnetic measurement data (Fig. 4a). The two-step shape of the $R(T)$ dependences in external magnetic fields (Fig. 4b) is typical of granular HTSs [1, 9, 10, 18–20, 22, 26, 29, 32–35, 37, 45, 48–57] and reflects the presence of two superconducting subsystems in these objects. Here, the sharp resistance drop corresponds to the transition in grains and the extended tail reflects the dissipation processes occurring in the subsystem of grain boundaries. The value of the smooth $R(T)$ portion in different external fields at the beginning of their significant divergence corresponds to the resistance of the subsystem of

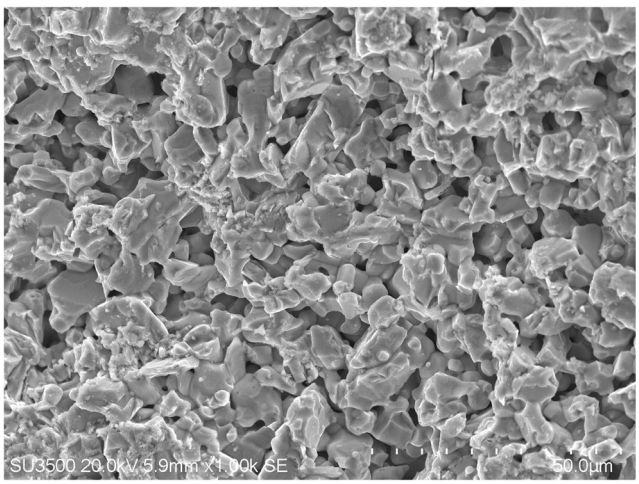

Fig. 2 Typical scanning electron microscopy image of the investigated $YBa_2Cu_3O_{7-\delta}$ sample

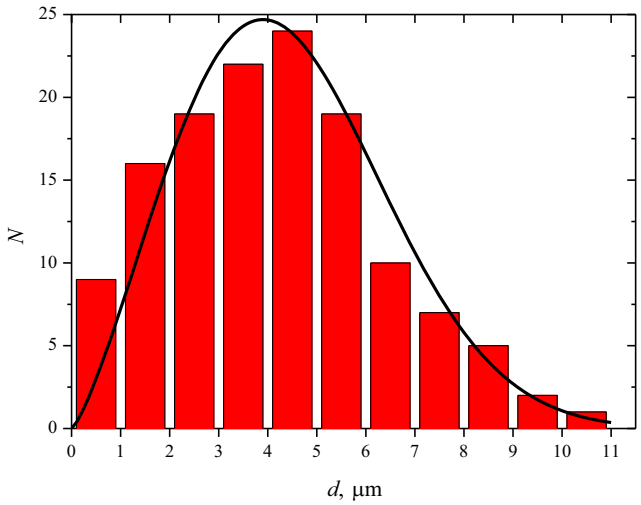

Fig. 3 Size distribution of grains. The line shows the Weibull distribution, which is best appropriate for milled materials, for a dimensionless shape parameter of 2.3 and a scale parameter of 5.0 μm

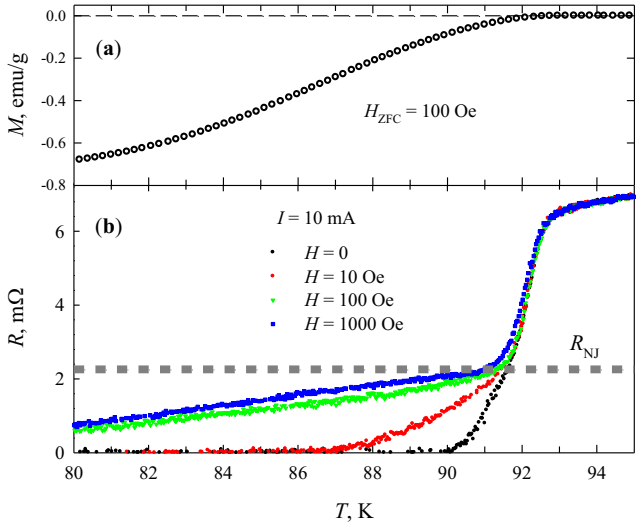

Fig. 4 Temperature dependences of **a** the magnetization in a field of 100 Oe (ZFC mode) and **b** the electrical resistance in zero fields and in fields of 10, 100, and 1000 Oe under the ZFC conditions. The horizontal dashed line in **b** corresponds to the resistance R_{NJ} of the subsystem of grain boundaries

grain boundaries (or their "normal" resistance) indicated as R_{NJ} in Fig. 4b.

The $M(H)$ magnetization hysteresis loops, as well as the virgin magnetization curve, at $T = 4.2$ K and 77 K are shown in Fig. 5 and the insets to it. The magnetic hysteresis loops are essentially asymmetric relative to the abscissa axis. This is typical of granular HTSs and is explained by the weak pinning of vortices in the surface layer of grains [58]. The current circulation scale D_c was estimated from the observed asymmetry of the magnetization hysteresis loop. According to [59], we have

$$D_c \approx 2\lambda_L(T) / \left[1-(\Delta M/2|M(H_{inc})|)^{1/3}\right] \quad (4)$$

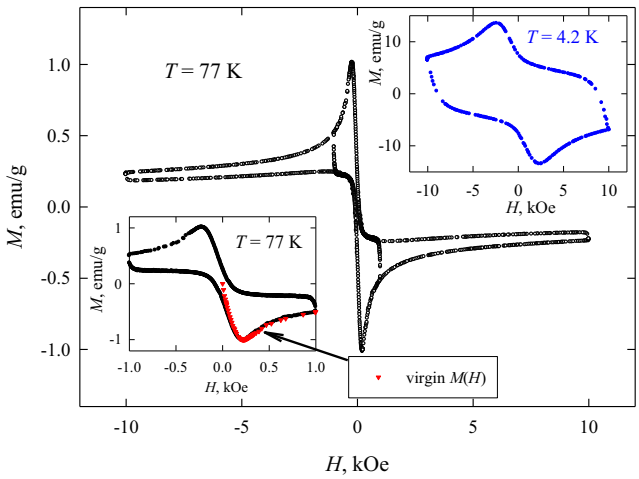

Fig. 5 Magnetization hysteresis loops for the investigated sample at T = 77 K. Upper inset: $M(H)$ at $T = 4.2$ K. Lower inset: $M(H)$ in the range of ± 1 kOe and the virgin magnetization under the ZFC conditions at $T = 77$ K

where λ_L is the depth of the magnetic field penetration into the investigated superconductor at the measuring temperature, $\Delta M = M(H_{dec}) - M(H_{inc})$, H_{inc} is the increasing field, and H_{dec} is the decreasing field. In the estimation of the D_c value using Eq. (4), the $M(H_{dec})$ and $M(H_{inc})$ values are taken at $H_{dec} = H_{inc} = H_m$, where H_m is the minimum field in the $M(H_{inc})$ dependence. The obtained circulation scale (3–4 μm) corresponds to the circulation in the sample grains.

The intergrain critical current density J_{CG} was determined from the magnetization hysteresis loop using the critical state model [60]. For polycrystalline superconductors, the relation between J_{CG} and ΔM is written as follows [58]:

$$J_{CG}\left(\mathrm{A/cm^2}\right) = 30\ \Delta M\left(\mathrm{emu/cm^3}\right)/d(\mathrm{cm}) \quad (5)$$

where d is the average grain size. Given $d \sim 4$ μm, the J_{CG} values in an external field of $H \approx 100$ Oe were found to be ~ 5.6×10^4 A/cm^2 at 77 K and ~ 7.4×10^6 A/cm^2 at 4.2 K. The obtained values show a great difference between the critical current densities in the superconducting subsystems (grains and grain boundaries) mentioned in Section 1. The presented data show that the sample under study exhibits the properties typical of granular HTSs of the yttrium system.

4 Magnetoresistance Hysteresis and Its Width

Figure 6 shows the hysteretic $R(H)$ dependences obtained at temperatures of 77 K and 4.2 K and transport currents of 300 and 35 mA (at $T = 77$ K). The presented $R(H)$ dependences were recorded upon field cycling within ± 10 and ± 1 kOe (at $T = 77$ K), except for the initial magnetoresistance behavior (starting with $H = 0$ after meeting the ZFC conditions). To give an example of the description of the hysteretic

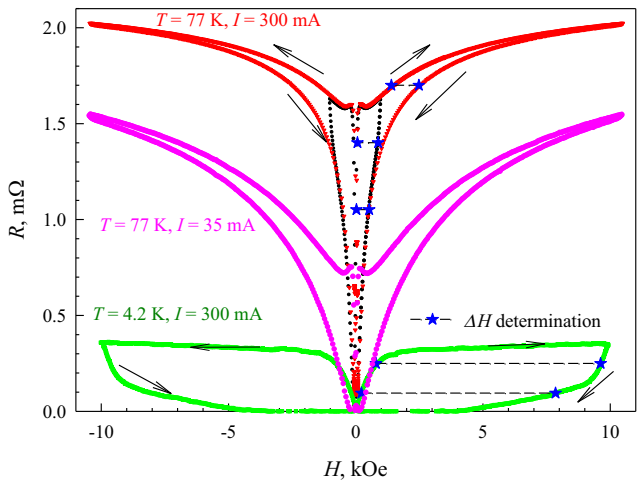

Fig. 6 Hysteretic $R(H)$ dependences at the indicated temperatures and transport currents I. Arrows show the external field variation. Horizontal dashed lines give examples of the determination of the magnetoresistance hysteresis width ΔH

magnetoresistance behavior, Fig. 7a shows a portion of the $R(H)$ dependence at $T = 77$ K upon field cycling within ± 1 kOe, which includes the initial dependence on $H_{inc} = 0$ (after meeting the ZFC conditions). For these data, the thermomagnetic prehistory fully corresponds to the $M(H)$ dependence shown in the lower inset to Fig. 5. It should be noted that the resistance at a current of $I = 300$ mA, a field of $H = 10$ kOe, and a temperature of 77 K does not exceed the R_{NJ} value (see Fig. 4b), being close to it though. This shows once again that the dissipation observed under the experimental conditions (Figs. 6 and 7a) only occurs in grain boundaries.

Figure 7b shows the dependence of the effective field $B_{eff}(H)$ in the intergrain medium plotted using the abovementioned $M(H)$ data by Eq. (2). The α value was selected to ensure the best agreement between the $R(H)$ and $B_{eff}(H)$ hysteresis widths. This comparison is reasoned by the following. For $R(H_{inc}) = R(H_{dec})$, the effective fields should be identical $B_{eff}(H_{inc}) = B_{eff}(H_{dec})$ at the fields H_{inc} and H_{dec} (Eqs. (2) and (3)). The hysteresis width ΔH is, in fact, the length of the segment $H_{dec} - H_{inc}$ when $R(H_{dec}) = R(H_{inc})$ for the magnetoresistance (Figs. 6 and 7a) or when $B_{eff}(H_{dec}) = B_{eff}(H_{inc})$ for the effective field (Fig.7b). The segments $\Delta H = H_{dec} - H_{inc}$ are shown in Figs. 6 and 7 by horizontal dashed lines. In Fig. 7, one can see good agreement between the $R(H)$ and $B_{eff}(H)$ dependences. Here, we mean both the relative positioning of different branches of the hysteresis loops relative to their initial dependences and the presence of the local maximum (in the increasing field) and minimum (in the decreasing field). In addition, the described approach explains both the nonzero remanent resistance $R_{rem} \equiv R(H_{dec} = 0)$, which corresponds to the nonzero value of $B_{eff}(H_{dec} = 0)$ caused by the remanent magnetization (the magnetic flux captured by HTS grains) in zero fields (Fig. 5). At the data in Fig. 7b, the parameter α equals 24 that is indicative of the strong magnetic flux compression in the intergrain medium [47, 50–55].

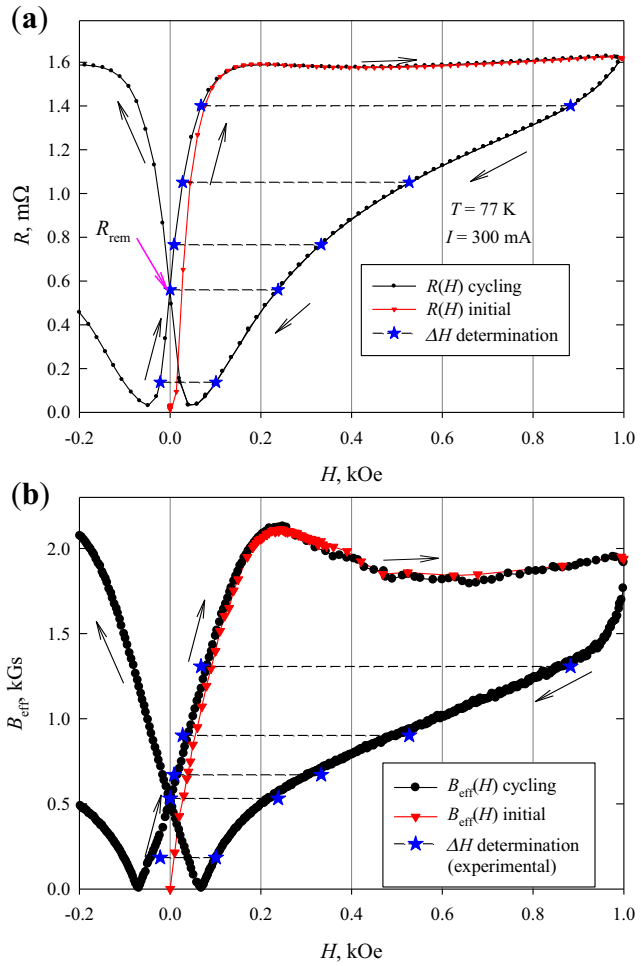

Fig. 7 Initial behavior and hysteresis of the magnetoresistance $R(H, I =$ 300 mA) (**a**) and the effective field *B*eff(*H*) (**b**) at $T = 77$ K. The *B*eff(*H*) dependences are plotted by Eq. (2) using the magnetization data (lower inset to Fig. 5) for $\alpha = 24$. The horizontal lines correspond to the field width ΔH of the magnetoresistance hysteresis; the line matching in **a** and **b** indicates equivalence of ΔH values for the $R(H)$ and *B*eff(*H*) hysteretic dependences

Now, let us analyze the magnetoresistance hysteresis width under the condition $R = \text{const}$. Obviously, the hysteresis width $\Delta H(H_{dec})$ should be smaller than H_{dec}. However, in the field range where the inequality $R < R_{rem}$ is valid, it is reasonable to determine the hysteresis field width using already a portion of the branch in the negative field range ($-H_{dec}$), as shown in Fig.7a and b. Here, the $\Delta H(H_{dec})$ value is somewhat higher than the H_{dec} value. Figure 8 shows the $\Delta H(H_{dec})$ dependences obtained in this way from the experimental $R(H)$ data at $T = 77$ K ($I = 35$ and 300 mA) and $T = 300$ K ($I = 300$ mA). Certainly, as we mentioned above, in a fairly wide field range, we have $\Delta H(H_{dec}) < H_{dec}$, which is illustrated in the inset to Fig. 8 for the data at 77 K. The striking thing in Fig. 8 is the proximity of the experimental $\Delta H(H_{dec})$ data to the linear function $\Delta H(H_{dec}) = H_{dec}$ in a fairly wide H_{dec} range. This

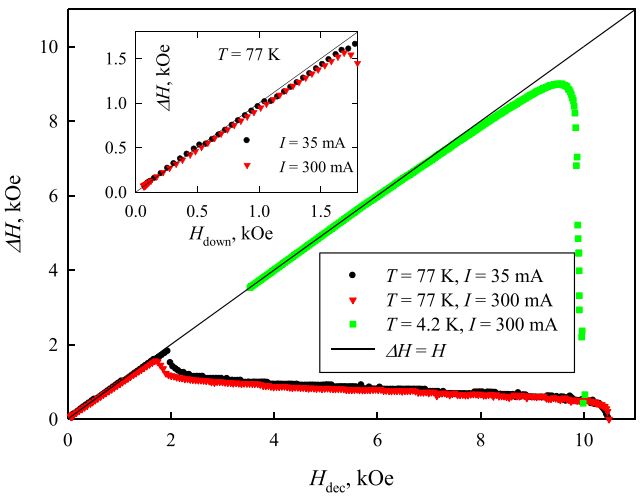

Fig. 8 Field width ΔH of the hysteresis. $\Delta H(H_{dec})$ pointes are obtained from the data presented in Fig. 6. The solid line shows the linear dependence $\Delta H = H$. Inset: data at $T = 77$ K in the weak-field region

points out that the field width of the hysteresis is close to its maximum value.

The behavior of the $\Delta H(H_{dec})$ dependence can be explained by the simple consideration of the shape of the $R(H)$ hysteresis. In Fig. 6, one can see the sharp $R(H_{inc})$ growth up to the field corresponding approximately to the $M(H_{inc})$ extremum (see Fig. 5). Then, the resistance growth with H_{inc} becomes much slower. In the decreasing field branch (the $R(H_{dec})$ dependence), the magnetoresistance drops fast in strong fields for the data at T = 4.2 K. For the data at T = 77 K, the $R(H_{dec})$ dependence sharply drops already in weak fields, while in strong fields, the magnetoresistance hysteresis is rather narrow. The $R(H)$ hysteresis width is zero in the maximum field, which is the end cycling point. As the field H_{dec} decreases, the $\Delta H(H_{dec})$ dependence can attain its maximum value fairly fast, which can be seen from the data at 4.2 K: the width ΔH is maximum already at H_{dec} ~ 9 kOe. For the data at 77 K, the maximum value is attained already in the much weaker field (H_{dec} ~ 2 kOe) since in the fields stronger than ~ 2 kOe, the $R(H)$ hysteresis is narrow. Nevertheless, in the H_{dec} range from 0 to a certain value (~ 1 kOe for the data at 77 K and ~ 6 kOe for the data at 4.2 K), we can speak about a certain universality of the $\Delta H(H_{dec})$ behavior. In point of fact, the $\Delta H(H_{dec})$ dependences obtained at the two temperatures that cover almost the entire range of the superconducting state are similar to the same linear function $\Delta H(H_{dec}) = H_{dec}$.

The described behavior can be explained using the following prerequisites. According to the critical state model [60], in an external field, screening currents circulate inside grains. A current density is equal to the critical current density. These currents induce a field in the intergrain medium (Fig. 1a and b), which increases due to the flux compression (Fig. 1c). This leads to the observed sharp resistance growth with increasing field H_{inc} (according to Eq. (3); see also Figs. 6 and 7a), at least up to the field of the $M(H)$ minimum. In addition, a significant change in the resistance can be observed for the decreasing field branch if the magnetization of grains changes fairly fast, e.g., at the change in the external field direction ($H_{inc} \rightarrow H_{dec}$) (see Figs. 6 and 7a). The analysis of the magnetic hysteresis loops made in Section 3 showed that the intragrain critical current density increases by almost two orders of magnitude as the temperature decreases from 77 to 4.2 K. This leads to an increase in the magnetization at low temperatures. Then, the contribution of the induced field to the effective field in the intergrain medium at H_{inc} = const will be greater at lower temperatures. The effective field is a superposition of two contributions: the induced field and the external field. Depending on the temperature and the values and directions of the external field sweep (H_{inc}, H_{dec}), these contributions can be in different ratios. A simple way of estimating the quantitative ratio between these contributions is to plot the

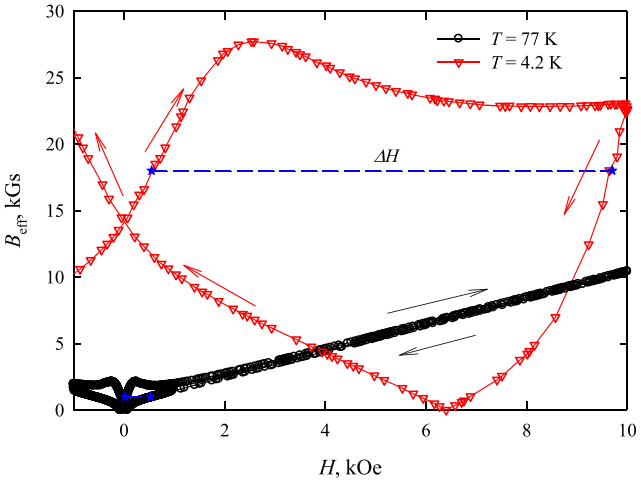

Fig. 9 Dependences $B_{eff}(H)$ of the effective field in the intergrain medium calculated using Eq. (2) for the data presented in Fig. 5 at α = 24. Horizontal lines correspond to the field width of the magnetoresistance hysteresis ΔH

$B_{eff}(H)$ dependence using Eq. (2). Figure 9 shows the $B_{eff}(H)$ dependences calculated using the experimental magnetization data (Fig. 5) and the above-obtained value α = 24. It is worth noting that, at low temperatures, the $B_{eff}(H)$ dependence yields only the qualitative agreement with the hysteretic behavior of the magnetoresistance. The quantitative agreement in strong fields at low temperatures can be obtained taking into account the field dependence of the parameter α [55]. Here, we examine the $B_{eff}(H)$ dependences only to explain the functional $\Delta H(H_{dec})$ dependence. It can be seen in Fig. 9 that, at T = 4.2 K, the $B_{eff}(H)$ hysteresis is fairly wide over the entire field range, while at T = 77 K, the hysteresis is wide only in fields below 1–2 kOe. This is caused by the different contributions of the terms from Eq. (2) to the effective field. Indeed, for the data at T = 77 K, we have $B_{eff}(H = 10\ kOe) \approx 10$ kGs, i.e., $B_{eff} \approx H$ in strong fields, while for the data at T = 4.2 K, $B_{eff}(H = 10\ kOe) \sim 20$ kGs, i.e., $B_{eff} > H$. The analysis of the data presented in Figs. 7b and 9 shows the validity of the strict inequality $B_{eff}(H_{inc}) >> H_{inc}$ in the field range from H_{inc} = 0 to the $B_{eff}(H_{inc})$ maximum at least. In this portion of the increasing field branch, the magnetoresistance sharply increases. At the same time, the portion of the sharp drop of the effective field and, consequently, of the magnetoresistance in the decreasing field branch (Figs. 6 and 7a) leads to the large field width ΔH of the hysteresis. Thus, it is the great contribution of the term $\alpha \cdot 4\pi M(H,T)$ to the effective field (Eq. (2)) that ensures the wide magnetoresistance hysteresis and its almost linear functional dependence ($\Delta H \approx H$, Fig. 8) in a fairly wide field range.

In Fig. 10, the $\Delta H(H_{dec})$ dependences are normalized to the field H_m corresponding to the $M(H_{inc})$ minimum. The field H_m also approximately corresponds to the $B_{eff}(H_{inc})$ (Figs. 7b and 9) and $R(H_{inc})$ maxima (Fig. 7a). It can be seen in Fig. 10 that the hysteresis width is most close to the linear dependence

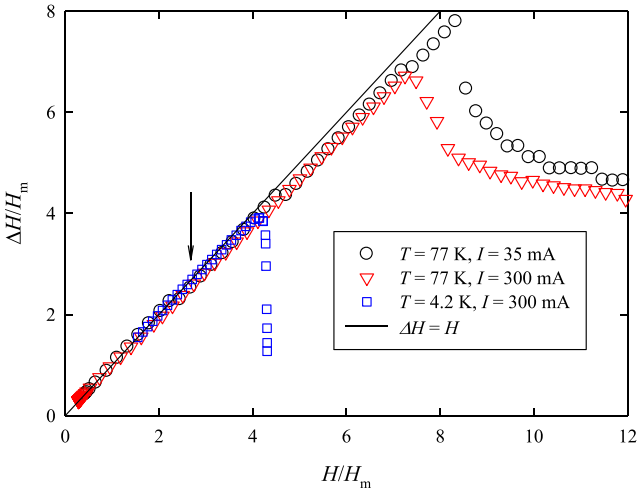

Fig. 10 Dependences of ΔH on H_{dec} (for the data from Fig. 8) normalized along the abscissa and ordinate axes and on H_m = 2300 Oe at T = 4.2 K and H_m = 231 Oe at T = 77 K. The solid line shows the dependence $\Delta H = H$. The arrow shows the point at which the $\Delta H(H_{dec})$ dependence follows approximately the dependences $\Delta H = H$

$\Delta H \approx H$ in the range of up to $H \approx 3H_m$. This value correlates well with the depth of full penetration of the magnetic field into a superconductor, which is estimated from the $M(H)$ dependences [61, 62]. Certainly, it is difficult to establish a clear criterion for the deviation of the $\Delta H(H_{dec})$ dependence from a linear function, but the full penetration field is also problematic to be accurately determined [61]. In this case, we are speaking about the field of complete penetration into HTS grains, which have the size distribution (Fig. 3). In view of the aforesaid, we can state that there is a correlation between the external field range in which the $R(H)$ hysteresis width takes its maximum value and the field range in which the field has not fully penetrated into HTS grains yet. This additionally confirms the concept of an effective field in the intergrain medium, where a large, sometimes dominant, contribution is made by the magnetic response of HTS grains, which results in a very wide hysteresis ($\Delta H \approx H$) in the external fields from 0 to $3H_m$.

5 Conclusions

Granular HTSs exhibit a fairly wide $R(H)$ magnetoresistance hysteresis. This hysteresis and its form are explained by the concept of an effective field in the intergrain medium taking into account the effect of the magnetic response of HTS grains to the field in the intergrain medium.

The $R(H)$ dependences obtained on the yttrium HTS sample demonstrate a universal behavior, specifically, the almost linear dependence of the magnetoresistance hysteresis width ΔH on the field H_{dec} (for the descending hysteresis branch) with the same slope $\Delta H \approx H_{dec}$ at various temperatures (77 K and 4.2 K).

In fact, the hysteresis width takes almost the maximum possible value; this is observed in a fairly wide range of fields H_{dec} or, to be exact, approximately up to $3H_m$, where H_m corresponds to the extremum (the minimum for the increasing field branch in $M(H)$) of the magnetic hysteresis loop. The field $3H_m$ is considered to be the field of full penetration into HTS grains (taking into account the size distribution). Consequently, there is an interrelation between the observed functional dependence of the magnetoresistance hysteresis width and the processes of field penetration into grains. In addition, the wide magnetoresistance hysteresis is directly related to the magnetic flux compression in the intergrain medium, due to which the field induced by the magnetic moments of HTS grains (or, in fact, by intragrain currents) is significantly increased.

In view of the aforesaid, it would be reasonable to investigate the interplay between the morphology of superconducting grains and the functional dependence of the magnetoresistance hysteresis width in granular HTSs from yttrium and other (lanthanum, bismuth, etc.) systems. This will be the object of our further research.

Acknowledgments The authors are grateful to A.V. Shabanov for conducting the scanning electron microscopy, which was carried out on the equipment of the Krasnoyarsk Regional Center for Collective Use, Krasnoyarsk Scientific Center, Siberian Branch, Russian Academy of Sciences.

References

1. Dubson, M.A., Herbet, S.T., Calabrese, J.J., Harris, D.C., Patton, B.R., Garland, J.C.: Non-Ohmic dissipative regime in the superconducting transition of polycrystalline $Y_1Ba_2Cu_3O_x$. Phys. Rev. Lett. **60**, 1061 (1988). https://doi.org/10.1103/PhysRevLett.60.1061
2. Chaudhari, P., Mannhart, J., Dimos, D., Tsuei, C.C., Chi, J., Oprysko, M.M., Scheuermann, M.: Direct measurement of the superconducting properties of single grain boundaries in $Y_1Ba_2Cu_3O_{7-\delta}$. Phys. Rev. Lett. **60**, 1653 (1988). https://doi.org/10.1103/PhysRevLett.60.1653
3. Evetts, J.E., Glowacki, B.A.: Relation of critical current irreversibility to trapped flux and microstructure in polycrystalline $YBa_2Cu_3O_7$. Cryogenics. **28**, 641 (1988). https://doi.org/10.1016/0011-2275(88)90147-6
4. De Vries, J.W.C., Stolmann, G.M., Gijs, M.A.M.: Analysis of the critical current density in high-T_c superconducting films. Physica C. **157**, 406 (1989). https://doi.org/10.1016/0921-4534(89)90264-5
5. Petrov, M.I., Krivomazov, S.N., Khrustalev, B.P., Aleksandrov, K.S.: A study of the hysteresis property of the current-voltage characteristic in high-temperature superconductors. Solid State Commun. **82**, 453 (1992). https://doi.org/10.1016/0038-1098(92)90748-X
6. Altshuler, E., Musa, J., Barroso, J., Papa, A.R.R., Venegas, V.: Generation of $J_c(H_e)$ hysteresis curves for granular $YBa_2Cu_3O_{7-\delta}$ superconductors. Cryogenics. **33**, 308 (1993). https://doi.org/10.1016/0011-2275(93)90051-O
7. Ji, L., Rzchowski, M.S., Anand, N., Tinkham, M.: Magnetic-field-dependent surface resistance and two-level critical-state model for

granular superconductors. Phys. Rev. B. **47**, 470 (1993). https://doi.org/10.1103/PhysRevB.47.470
8. Wright, A.C., Zhang, K., Erbil, A.: Dissipation mechanism in a high-Tc granular superconductor: applicability of a phase-slip model. Phys. Rev. B. **44**, 863 (1991). https://doi.org/10.1103/PhysRevB.44.863
9. Gaffney, C., Petersen, H., Bednar, R.: Phase-slip analysis of the non-Ohmic transition in granular $YBa_2Cu_3O_{6.9}$. Phys. Rev. B. **48**, 3388 (1993). https://doi.org/10.1103/PhysRevB.48.3388
10. Gamchi, H.S., Russel, G.J., Taylor, K.N.R.: Resistive transition for $YBa_2Cu_3O_{7-\delta}$-Y_2BaCuO_5 composites: influence of a magnetic field. Phys. Rev. B. **50**, 12950 (1994). https://doi.org/10.1103/PhysRevB.50.12950
11. Soulen, R.J., Francavilla, T.L., Fuller-Mora, W.W., Miller, M.M., Joshi, C.H., Carter, W.L., Rodenbush, A.J., Manlief, M.D., Aized, D.: Explanation of the dissipation observed in several high-temperature superconductors using a modified Ambegaokar-Halperin model. Phys. Rev. B. **50**, 478 (1994). https://doi.org/10.1103/PhysRevB.50.478
12. Liebenberg, D.H., Soulen, R.J., Francavilla, T.L., Fuller-Mora, W.W., McIntyre, P.C., Cima, M.J.: Current-voltage measurements of thin $YBa_2Cu_3O_{6.9}$ films compared with a modified Ambegaokar-Halperin theory. Phys. Rev. B. **51**, 11838 (1995). https://doi.org/10.1103/PhysRevB.51.11838
13. Soulen, R.J., Francavilla, T.L., Drews, A.R., Toth, L., Osofsly, M.S., Lechter, W.L., Skelton, E.F.: Transport studies of bulk $Pb_{0.2}Hg_{0.8}Ba_2Ca_{1.75}Cu_3O_x$. Phys. Rev. B. **51**, 1393 (1995). https://doi.org/10.1103/PhysRevB.51.1393
14. Joshi, R.J., Hallock, R.B., Taylor, J.A.: Critical exponents of the superconducting transition in granular $YBa_2Cu_3O_{7-\delta}$. Phys. Rev. B. **55**, 9107 (1997). https://doi.org/10.1103/PhysRevB.55.9107
15. Mohammadizadeh, M.R., Akhavan, M.: Thermally activated flux creep in the $Gd(Ba_{2-x}Pr_x)Cu_3O_{7+\delta}$ system. Supercond. Sci. Technol. **16**, 538 (2003). https://doi.org/10.1088/0953-2048/16/4/320
16. Shakeripour, H., Akhavan, M.: Thermally activated phase-slip in high-temperature cuprates. Supercond. Sci. Technol. **14**, 234 (2001). https://doi.org/10.1088/0953-2048/14/5/302
17. Urba, L., Acha, C., Bekeris, V.: Dissipation mechanisms in granular high T_c superconductors. Physica C. **279**, 92 (1997). https://doi.org/10.1016/S0921-4534(97)00168-8
18. Petrov, M.I., Balaev, D.A., Shaikhutdinov, K.A., Aleksandrov, K.S.: Influence of transport current and thermal fluctuations on the resistive properties of HTSC+CuO composites. Phys. Solid State. **41**, 881 (1999). https://doi.org/10.1134/1.1130895
19. Petrov, M.I., Balaev, D.A., Shaikhutdinov, K.A., Aleksandrov, K.S.: Superconductor-semiconductor-superconductor junction network in bulk polycrystalline composites $Y_{3/4}Lu_{1/4}Ba_2Cu_3O_7 + Cu_{1-x}Li_xO$. Supercond. Sci. Technol. **14**, 798 (2001). https://doi.org/10.1088/0953-2048/14/9/333
20. Bhalla, G.L., Pratima, Malik, A., Singh, K.K.: Dissipation mechanism in a high-T_c $Bi_{1.7}Pb_{0.3}Sr_2Ca_2Cu_3O_x$ granular superconductor. Physica C. **391**, 17 (2003). https://doi.org/10.1016/S0921-4534(03)00805-0
21. Albiss, B.A.: Thick films of superconducting YBCO as magnetic sensors. Supercond. Sci. Technol. **18**, 1222 (2005). https://doi.org/10.1088/0953-2048/18/9/014
22. Bhalla, G.L., Pratima: Vortex–antivortex behaviour and thermally activated phase slip in a polycrystalline $YBa_2Cu_3O_{7-\delta}$ superconductor. Supercond. Sci. Technol. **20**, 1120 (2007). https://doi.org/10.1088/0953-2048/20/12/006
23. Quian, Y.J., Tang, Z.M., Chen, K.Y., Zhou, B., Qui, J.W., Miao, B.C., Cai, Y.M.: Transport hysteresis of the oxide superconductor $Y_1Ba_2Cu_3O_{7-x}$ in applied fields. Phys. Rev. B. **39**, 4701 (1989). https://doi.org/10.1103/PhysRevB.39.4701
24. Celasco, M., Masoero, A., Mazzetti, P., Stepanescu, A.: Evidence of current-noise hysteresis in superconducting YBa2Cu3O7−δ specimens in a magnetic field. Phys. Rev. B. **44**, 5366 (1991). https://doi.org/10.1103/PhysRevB.44.5366
25. Lopez, D., de la Cruz, F.: Anisotropic energy dissipation in high-Tc ceramic superconductors: Local-field effects. Phys. Rev. B. **43**, 11478 (1991). https://doi.org/10.1103/PhysRevB.43.11478
26. Lopez, D., Decca, R., de la Cruz, F.: Anisotropic energy dissipation, flux flow and topological pinning in ceramic superconductors. Supercond. Sci.Technol. **5**, 276 (1992). https://doi.org/10.1088/0953-2048/5/1S/061
27. Kilic, A., Kilic, K., Senoussi, S., Demir, K.: Influence of an external magnetic field on the current–voltage characteristics and transport critical current density. Physica C. **294**, 203 (1998). https://doi.org/10.1016/S0921-4534(97)01687-0
28. Gerashchenko, O.V., Ginzburg, S.L.: Angular dependence of current-voltage characteristics and voltage fluctuation spectrum in granular superconductors. Supercond. Sci. Technol. **13**, 332 (2000). https://doi.org/10.1088/0953-2048/13/3/311
29. Balaev, D.A., Prus, A.G., Shaukhutdinov, K.A., Gokhfeld, D.M., Petrov, M.I.: Study of dependence upon the magnetic field and transport current of the magnetoresistive effect in YBCO-based bulk composites. Supercond. Sci. Technol. **20**, 495 (2007). https://doi.org/10.1088/0953-2048/20/6/002
30. Derevyanko, V.V., Sukhareva, T.V., Finkel, V.A.: Penetration of a magnetic field into the $YBa_2Cu_3O_{7-\delta}$ high-temperature superconductor: Magnetoresistance in weak magnetic fields. Phys. Solid State. **46**, 1798 (2004). https://doi.org/10.1134/1.1809408
31. Kuz'michev, N.D.: Critical state of Josephson medium. JETP Lett. **74**, 262 (2001). https://doi.org/10.1134/1.1417162
32. Daghero, D., Mazzetti, P., Stepanescu, A., Tura, P.: Electrical anisotropy in high-Tc granular superconductors in a magnetic field. Phys. Rev. B. **66**, 11478 (2002). https://doi.org/10.1103/PhysRevB.66.184514
33. Mune, P., Fonseca, F.C., Muccillo, R., Jardim, R.F.: Magnetic hysteresis of the magnetoresistance and the critical current density in polycrystalline $YBa_2Cu_3O_{7-\delta}$–Ag superconductors. Physica C. **390**, 363 (2003). https://doi.org/10.1016/S0921-4534(03)00802-5
34. Balaev, D.A., Gokhfeld, D.M., Dubrovskii, A.A., Popkov, S.I., Shaykhutdinov, K.A., Petrov, M.I.: Magnetoresistance hysteresis in granular HTSCs as a manifestation of the magnetic flux trapped by superconducting grains in YBCO + CuO composites. JETP. **105**, 1174 (2007). https://doi.org/10.1134/S1063776107120084
35. Balaev, D.A., Dubrovskii, A.A., Shaykhutdinov, K.A., Popkov, S.I., Gokhfeld, D.M., Gokhfeld, Y.S., Petrov, M.I.: Mechanism of the hysteretic behavior of the magnetoresistance of granular HTSCs: the universal nature of the width of the magnetoresistance hysteresis loop. JETP. **108**, 241 (2009). https://doi.org/10.1134/S106377610902006X
36. Blatter, G., Feigel'man, M.V., Gekshkebein, V.B., Larkin, A.I., Vinokur, V.M.: Vortices in high-temperature superconductors. Rev. Mod. Phys. **66**, 1125 (1994). https://doi.org/10.1103/RevModPhys.66.1125
37. Semenov, S.V., Balaev, A.D., Balaev, D.A.: Dissipation in granular high-temperature superconductors: new approach to describing the magnetoresistance hysteresis and the resistive transition in external magnetic fields. J. Appl. Phys. **125**, 033903 (2019). https://doi.org/10.1063/1.5066602
38. Palau, A., Puig, T., Obradors, X., Pardo, E., Navau, C., Sanchez, A., Usoskin, A., Freyhardt, H.C., Fernández, L., Holzapfel, B., Feenstra, R.: Simultaneous inductive determination of grain and intergrain critical current densities of $YBa_2Cu_3O_{7-x}$ coated conductors. Appl. Phys. Lett. **84**, 230 (2004). https://doi.org/10.1063/1.1639940
39. Derevyanko, V.V., Sukhareva, T.V., Finkel, V.A.: Magnetoresistance hysteresis of granular $YBa_2Cu_3O_{7-\delta}$ high-

temperature superconductor in weak magnetic fields. Tech. Phys. **53**, 321 (2008). https://doi.org/10.1134/S1063784208030067
40. Sukhareva, T.V., Finkel, V.A.: Hysteresis of the magnetoresistance of granular HTSC $YBa_2Cu_3O_{7-\delta}$ in weak fields. Phys. Solid State. **50**, 1001 (2008). https://doi.org/10.1134/S1063783408060012
41. Balaev, D.A., Semenov, S.V., Petrov, M.I.: Dominant influence of the compression effect of a magnetic flux in the intergranular medium of a granular high-temperature superconductor on dissipation processes in an external magnetic field. Phys. Solid State. **55**, 2422 (2013). https://doi.org/10.1134/S1063783413120044
42. Sukhareva, T.V., Finkel, V.A.: Phase transition in the vortex structure of granular $YBa_2Cu_3O_{7-\delta}$ HTSCs in weak magnetic fields. JETP. **107**, 787 (2008). https://doi.org/10.1134/S1063776108110083
43. Altinkok, A., Kilic, K., Olutas, M., Kilic, A.: Magnetovoltage measurements and hysteresis effects in polycrystalline superconducting $Y_1Ba_2Cu_3O_{7-x}$ /Ag in weak magnetic fields. J. Supercond. Nov. Magn. **26**, 3085 (2013). https://doi.org/10.1007/s10948-013-2139-y
44. Derevyanko, V.V., Sukhareva, T.V., Finkel, V.A., Shakhov, Y.N.: Effect of temperature and magnetic field on the evolution of a vortex structure of the granular $YBa_2Cu_3O_{7-\delta}$ high-temperature superconductor. Phys. Solid State. **56**, 649 (2014). https://doi.org/10.1134/S1063783414040076
45. Derevyanko, V.V., Sukhareva, T.V., Finkel, V.A.: Phase transitions and vortex structure evolution in two-level high-temperature granular superconductor $YBa_2Cu_3O_{7-\delta}$ under temperature and magnetic field. Phys. Solid State. **59**, 1492 (2017). https://doi.org/10.1134/S1063783417080091
46. Balaev, D.A., Popkov, S.I., Semenov, S.V., Bykov, A.A., Shaykhutdinov, K.A., Gokhfeld, D.M., Petrov, M.I.: Magnetoresistance hysteresis of bulk textured $Bi_{1.8}Pb_{0.3}Sr_{1.9}Ca_2Cu_3O_x$ + Ag ceramics and its anisotropy. Physica C. **470**, 61 (2010). https://doi.org/10.1016/j.physc.2009.10.007
47. Balaev, D.A., Popkov, S.I., Sabitova, E.I., Semenov, S.V., Shaykhutdinov, K.A., Shabanov, A.V., Petrov, M.I.: Compression of a magnetic flux in the intergrain medium of a $YBa_2Cu_3O_7$ granular superconductor from magnetic and magnetoresistive measurements. J. Appl. Phys. **110**, 093918 (2011). https://doi.org/10.1063/1.3657775
48. Derevyanko, V.V., Sukhareva, T.V., Finkel, V.A.: Effect of the temperature, external magnetic field, and transport current on electrical properties, vortex structure evolution processes, and phase transitions in subsystems of superconducting grains and "weak links" of granular two-level high-temperature superconductor $YBa_2Cu_3O_{7-\delta}$. Phys. Solid State. **60**, 470 (2018). https://doi.org/10.1134/S1063783418030083
49. Balaev, D.A., Bykov, A.A., Semenov, S.V., Popkov, S.I., Dubrovskii, A.A., Shaykhutdinov, K.A., Petrov, M.I.: General regularities of magnetoresistive effects in the polycrystalline yttrium and bismuth high-temperature superconductor systems. Phys. Solid State. **53**, 922 (2011). https://doi.org/10.1134/S1063783411050052
50. Semenov, S.V., Balaev, D.A.: Model of the behavior of a granular HTS in an external magnetic field: temperature evolution of the magnetoresistance hysteresis. Phys. Solid State. **62**, 1136 (2020). https://doi.org/10.1134/S1063783420070239
51. Balaev, D.A., Semenov, S.V., Petrov, M.I.: J. Supercond. Nov. Magn. **27**, 1425 (2014)
52. Semenov, S.V., Balaev, D.A., Pochekutov, M.A., Velikanov, D.A.: Anisotropy of the magnetoresistive properties of granular high-temperature superconductors resulting from magnetic flux compression in the intergrain medium. Phys. Solid State. **59**, 1291 (2017). https://doi.org/10.1134/S1063783417070241
53. Balaev, D.A., Semenov, S.V., Pochekutov, M.A.: Anisotropy of the magnetoresistance hysteresis in the granular superconductor Y-Ba-Cu-O at different magnetic-field and transport-current orientations. J. Appl. Phys. **122**, 123902 (2017). https://doi.org/10.1063/1.4986253
54. Semenov, S.V., Balaev, D.A.: Temperature behavior of the magnetoresistance hysteresis in a granular high-temperature superconductor: magnetic flux compression in the intergrain medium. Physica C. **550**, 19 (2018). https://doi.org/10.1016/j.physc.2018.04.005
55. Semenov, S.V., Balaev, D.A.: Magnetoresistance hysteresis evolution in the granular Y–Ba–Cu–O high-temperature superconductor in a wide temperature range. J. Supercond. Nov. Magn. **32**, 2409 (2019). https://doi.org/10.1007/s10948-019-5043-2
56. dos Santos, C.A.M., da Luz, M.S., Machado, A.J.S.: On the transport properties in granular or weakly coupled superconductors. Physica C. **391**, 345 (2003). https://doi.org/10.1016/S0921-4534(03)00963-8
57. Balaev, D.A., Popkov, S.I., Semenov, S.V., Bykov, A.A., Sabitova, E.I., Dubrovskiy, A.A., Shaikhutdinov, K.A., Petrov, M.I.: Contributions from inter-grain boundaries to the magneto-resistive effect in polycrystalline high-T superconductors. The underlying reason of different behavior for YBCO and BSCCO systems. J. Supercond. Nov. Magn. **24**, 2129 (2011). https://doi.org/10.1007/s10948-011-1166-9
58. Gokhfeld, D.M.: An extended critical state model: asymmetric magnetization loops and field dependence of the critical current of superconductors. Phys. Solid State. **56**, 2380 (2014). https://doi.org/10.1134/S1063783414120129
59. Gokhfeld, D.M.: The circulation radius and critical current density in type II superconductors. Tech. Phys. Lett. **45**, 1 (2019). https://doi.org/10.1134/S1063785019010243
60. Bean, C.P.: Magnetization of high-field superconductors. Rev. Mod. Phys. **36**, 31 (1964). https://doi.org/10.1103/RevModPhys.36.31
61. Yeshurun, Y., Malozemoff, A.P., Shaulov, A.: Magnetic relaxation in high-temperature superconductors. Rev. Mod. Phys. **68**, 911 (1996). https://doi.org/10.1103/RevModPhys.68.911
62. Gokhfeld, D.M.: Critical current density and trapped field in HTS with asymmetric magnetization loops. J. Phys. Conf. Ser. **695**, 012008 (2016). https://doi.org/10.1088/1742-6596/695/1/012008